Available online at www.sciencedirect.com
SCIENCE DIRECT
Biochimica et Biophysica Acta 1712 (2005) 161 – 172
BIOCHIMICA ET BIOPHYSICA ACTA
BBA
http://www.elsevier.com/locate/bba

Effects of cargo molecules on the cellular uptake of arginine-rich cell-penetrating peptides

James R. Maiolo[a,b], Marc Ferrer[b,*], Elizabeth A. Ottinger[a,1]

[a]Department of Chemistry and Biochemistry, Swarthmore College, 500 College Avenue, Swarthmore, PA, 19081, USA
[b]Department of Automated Biotechnology, Merck & Co., Merck Research Laboratories, 502 Louise Lane, North Wales, PA 19454, USA

Received 10 February 2005; received in revised form 1 April 2005; accepted 25 April 2005
Available online 17 May 2005

Abstract

The identification of cell-penetrating peptides (CPPs) as vectors for the intracellular delivery of conjugated molecules such as peptides, proteins, and oligonucleotides has emerged as a significant tool to modulate biological activities inside cells. The mechanism of CPP uptake by the cells is still unclear, and appears to be both endocytotic and non-endocytotic, depending on the CPP and cell type. Moreover, it is also unknown whether cargo sequences have an effect on the uptake and cellular distribution properties of CPP sequences. Here, we combine results from quantitative fluorescence microscopy and binding to lipid membrane models to determine the effect of cargo peptide molecules on the cellular uptake and distribution of the arginine-rich CPPs, R_7, and R_7W, in live cells. Image analysis algorithms that quantify fluorescence were used to measure the relative amount of peptide taken up by the cell, as well as the extent to which the uptake was endocytotic in nature. The results presented here indicate that fusion of arginine-rich CPPs to peptide sequences reduces the efficiency of uptake, and dramatically changes the cellular distribution of the CPP from a diffuse pattern to one in which the peptides are mostly retained in endosomal compartments.

Keywords: Conjugated cell-penetrating peptide; Arginine-rich peptide; Cellular distribution; Quantitative fluorescence microscopy; Endocytosis; Lipid binding

1. Introduction

Transduction of biologically active molecules across cell membranes to interact with intracellular targets is a persistent challenge. These membrane barriers are one of the major obstacles hindering the use of oligonucleotides and polypeptides as tools to study cellular processes, as well as the development of drug candidates. The identification of cell-penetrating peptides (CPPs) as vectors for the intracellular delivery of conjugated molecules such as peptides, proteins, and oligonucleotides has emerged as a powerful tool to modulate biological activities inside cells [1–4]. Several of the CPPs identified, such as pAntp-(43–58) [5] and Tat-(48–60) [6] are highly basic sequences derived from RNA- or DNA-binding proteins, while other CPPs, such as the oligoarginines (R_7 or R_9), have been artificially designed based on studies recognizing the importance of

Abbreviations: CPP, cell penetrating peptide; DIEA, diisopropylethylamine; DMEM, Dubelcco's Modified Eagle Medium; DMF, dimethylformamide; DMPC, dimyristoyl phosphatidylcholine; DMPG, dimyristoyl phosphidylglycerol; DMSO, dimethylsulfoxide; FBS, fetal bovine serum; Fl, 5-carboxyfluorescein; Fmoc, N-(9-fluorenyl)methoxycarbonyl; FP, fluorescence polarization; HBTU, 2-(1H-benzotriazole -1-yl)-1,1,3,3-tetramethyluronium hexafluorophosphate; HOBt, 1-hydroxybenzotriazole; NMP, *N*-methylpyrrolidinone; pAntp, antennapedia; PBS, phosphate-buffered saline; POPC, palmitoyl-oleoyl phosphatidylcholine; POPG, palmitoyl-oleoyl phosphatidylglycerol; SUV, small-unilamellar vesicles; TFA, trifluoroacetic acid

* Corresponding author. Tel.: +1 267 305 0251; fax: +1 267 305 3625.
E-mail address: marc−ferreralegre@merck.com (M. Ferrer).
[1] Current address: Department of Biochemistry and Biophysics, University of Pennsylvania, Clinical Research Building, 415 Curie Boulevard, Philadelphia, PA 19104, USA.

0005-2736/$ - see front matter © 2005 Elsevier B.V. All rights reserved.
doi:10.1016/j.bbamem.2005.04.010

positively charged arginines to mediate transport across cell membranes [7,8].

The mechanism by which these CPPs translocate across cell membranes is still not clearly understood. Initially, CPPs were found to enter cells by an energy independent, nonendocytotic process that was found to be fairly general across many different cell lines [5,8–15]. It was suggested that translocation across membranes was not receptor mediated since studies showed that the primary amino acid sequence was not important, and that D-amino acids could be substituted for the natural L-amino acids without affecting activity [7,10,14]. It was also found that these peptides, when conjugated to large cargo molecules such as polypeptides and oligonucleotides, would still translocate across the cell membrane and bring the cargo molecule into the cytoplasm and nucleus [16–20]. Many of the original experiments that monitored CPP uptake in cells were conducted using FACS sorting, or confocal microscopy of fluorescently labeled peptides in fixed cells. It is now known that these methods can prevent an accurate measurement of CPP cellular uptake, because FACS sorting cannot distinguish between peptide bound to the extracellular membrane, peptide present in intracellular vesicles, and peptide distributed evenly in the cytoplasm; and cell fixation for confocal microscopy studies causes artificial redistribution of CPPs from membranes and vesicles into the cytoplasm and nucleus [21–25].

Recent data using confocal microscopy with live cells show that the mechanism of uptake depends on the CPP sequence and cell type: for most CPPs, including pAntp, TAT-derived peptides, and other novel cell penetrating peptides such as sweet arrow peptide (SAT) and human calcitonin-derived peptide, the cellular uptake is energy dependent and endocytotic in nature [22,25–27]. For polyarginine sequences, it appears that peptides are taken up by a mixture of endocytotic and non-endocytotic processes [8,15,25,28]. Most of these live cell studies on cellular distribution and uptake have been done with the CPPs alone, and did not specifically examine the effect that conjugating biomolecules to the CPPs have on the uptake process. Since CPPs have been utilized for the transport of biomolecules into cells, it is therefore important to understand the uptake characteristics of CPPs attached to their cargo molecules. In this paper, we investigate the uptake characteristics of the CPPs, R_7, R_7W, and pAntp in U2OS (human oesteosarcoma) and A431 (human epidermoid carcinoma) cells, as well as the effect of conjugated peptide molecules on the uptake of R_7 and R_7W. Image analysis algorithms that quantify fluorescence from cellular vesicles were used to quantify the relative extent to which the uptake was endocytotic in nature. Our studies show that the patterns of distribution for CPPs alone in comparison to CPPs conjugated to peptides are different in live cells. In general, we found that CPPs alone show a varying degree of a mixture of diffuse cytoplasmic and nuclear staining, and punctate staining, and that the pattern of distribution varied considerably depending on the temperature and cell line. In contrast, CPPs conjugated to cargo peptides showed less efficiency of uptake, and almost exclusive punctate staining compared to the CPP alone.

One of the initial steps in the translocation of these positively charged CPPs has been postulated to be their interaction with the negatively charged lipids in the plasma membrane. In this regard, it has been found that the number of arginine residues has an effect on the efficiency and mode of cellular uptake [8,15]. In an attempt to understand whether the different uptake and distribution properties of the conjugated polyarginines compared to the CPPs alone could be related to an overall change in charge of the peptide, and as a consequence their ability to interact with the membrane, we studied the binding properties of these peptides to membrane models using fluorescence polarization. The lipid binding studies showed that all of the peptides bind to negatively charged lipids to some degree, and that conjugated polyarginines did not have significantly different binding properties compared to the CPPs by themselves. Therefore, binding to lipid models did not necessarily correlate with the uptake characteristics of the peptides in the cell lines tested. These results indicate that other properties, in addition to lipid binding, may be involved in the initial membrane binding and translocation process of the arginine-rich CPPs.

2. Materials and methods

2.1. General

Cell lines were obtained from ATCC: U2OS (CRL-2592) and A431NS (HTB-96). Fluorescein-RRRRRRRW-NH_2 (Fl-R_7W), fluorescein-HRRNEEVQDTRL-OH (Fl-DTRL), and fluorescein-RRRRRRR-GREEEVQDTRL-OH (Fl-R_7-DTRL) were purchased from SynPep (Dublin, CA). Dimyristoyl phosphatidylcholine (DMPC), dimyristoyl phosphidylglycerol (DMPG), palmitoyl-oleoyl phosphatidylcholine (POPC) and palmitoyl-oleoyl phosphatidylglycerol (POPG) were purchased from Avanti Polar Lipids, Inc. (Alabaster, AL). 5- carboxyfluorescein was from Molecular Probes (Eugene, OR). Fmoc-protected amino acid derivatives were from Peptides International (Louisville, KY) or SynPep (Dublin, CA). Other general reagents for peptide synthesis were from Fisher and Applied Biosystems.

2.2. Peptide synthesis and purification

Fluorescein-RRRRRRR-NH_2 (FL-R_7), Fluorescein-RQIKIWFQNRRMKWKK-NH_2 (Fl-pAntp), and fluorescein-RRRRRRRW-GREEEVQD-OH (Fl-R_7W-VQD) were synthesized using an Applied Biosystems 433A Peptide Synthesizer. The solid-phase synthesis was on TentaGel S PHB for c-terminus peptide acids or Fmoc-PAL resin for

the c-terminus peptide amides using Fmoc/*tert*-butyl chemistry. After synthesis was complete, fluorescein was coupled to the Fmoc deprotected *N*-terminus by reacting the resin with 4 equivalents of 5-carboxyfluorescein, 2-(1H-benzotriazole -1-yl)-1,1,3,3-tetramethyluronium hexafluorophosphate (HBTU), and 1-hydroxybenzotriazole (HOBt) and 8 eq diisopropylethylamine (DIEA) (4:4:4:8) in *N*-methylpyrolidine (NMP) for 16 h at RT in the dark. The resin was then washed with dimethylformamide (DMF), dichloromethane, and methanol (Table 1).

The peptides were cleaved form the resin with Reagent K, trifluoroacetic acid/phenol/H_2O/thioanisole/1,2-ethanedithiol (82.5:5:5:2.5, v/v/v/v) for 16 h except for FL-R_7 which was cleaved with trifluoroacetic acid/triisopropylsilane/H_2O (95:2.5:2.5, v/v/v) for 16h. The crude peptides were precipitated with diethyl ether (0 °C), collected by low speed centrifugation, washed with cold ether (3 times), dissolved in H_2O, and lyophilized. The peptides were purified by semipreparative reversed phase HPLC using a Vydac C-18 reversed-phase column (218TP510; 5μm, 10×250 mm) on a Breeze Waters system. The peptides were eluted with a linear gradient (5 ml/min) using 0.1% aqueous TFA/5% CH_3CN (Solvent A) and 0.1% TFA in CH_3CN (Solvent B) from 5 to 45% B over 40 min. The identity of the peptides was confirmed by electrospray ionization (ESI) mass spectrometry.

Peptide concentrations were determined by UV/Vis spectroscopy using a molar extinction coefficient for fluorescein of 66,000 M^{-1} cm^{-1} at 492 nm. Stock solutions of the fluorescein-labeled peptides were made in DMSO, and diluted in PBS to the concentrations used in the experiments.

2.3. Cell culture

All cells were grown at 37 °C in a 5% CO_2 atmosphere. U2OS cells were cultured in McCoy's 5A modified growth medium with 10% fetal bovine serum (FBS) to confluence and subcultured at a ratio of 1:4 to 1:10 by trypsin-EDTA dispersion. A431 cells were cultured in Dubelcco's Modified Eagle Medium, DMEM with 10% FBS to confluence and subcultured at a ratio of 1:10 by trypsin-EDTA dispersion.

Table 1
Peptide sequences utilized in this study[a]

Peptide	Sequence
R_7	Fl-RRRRRRR-NH_2
R_7W	Fl-RRRRRRRW-NH_2
pAntp	Fl-RQIKIWFQNRRMKWKK-NH_2
R_7-DTRL	Fl-RRRRRRRGREEEVQDTRL-OH
R_7W-VQD	Fl-RRRRRRRWGREEEVQD-OH
DTRL	Fl-HRRNEEVQDTRL-OH

[a] Three CPP sequences were chosen for this study because of their different proposed mechanism of uptake. pAntp has been shown to be internalized through an endocytotic mechanism. R_7 and R_7W are internalized by both endocytotic and non-endocytotic mechanisms. The peptide sequence fused to R_7 corresponds to the C-terminal fragment of the cystic fibrosis transmembrane conductance regulator (CFTR), and the sequence conjugated to R_7W, is a three amino acid deletion of the C-terminal fragment of the same protein. These sequences were chosen because of our interest in using these peptides for further biological studies.

Table 2
Image analysis parameters for the InCell 3000[a]

	U2OS		A431	
	Intensity	Granularity	Intensity	Granularity
Marker	Blue/Red	Blue/Red	Blue/Red	Blue/Red
Threshold	50/10+back	50/10+back	100/10+back	100/10+back
Discard	20% of peak	20% of peak	20% of peak	20% of peak
Bounding box	{9,250}	{9,250}	{9,250}	{9,250}
Signal	Green	Green	Green	Green
Dilation	7/11 pixels	7/11 pixels	3 pixels	6 pixels
Grain size	na	7 pixels	na	3 pixels
Gradient	na	1.2	na	1.15

[a] Numbers given as x/y are for the blue maker/red marker, respectively.

2.4. Peptide uptake experiments in live cells

U2OS cells were plated at 8000 cells per well overnight in 96-well Packard Viewplates (PerkinElmer, MA) in 100 μl growth medium (McCoy's 5A modified medium +10% FBS). A431 cells were similarly plated at a density of 15,000 cells per well. After overnight incubation, the media was removed and 100 μl fresh medium was added containing 180 μM propidium iodide and 5 μM Hoëchst 33258 for 30 min at 37 °C, followed by the addition 10 μl fluorescein labeled peptides (110 μM, in PBS with 4.7% DMSO), at 37 °C or 4 °C for 2 h. Cells were washed twice with 100 μl PBS, and fresh growth medium was added. Plates were then imaged using the InCell 3000 confocal microscope (GE Biosciences, NJ), and were kept at room temperature protected from light for the duration of imaging experiment. Images were captured by visualizing green fluorescence first (fluorescein-labeled peptide), followed by red fluorescence (propidium iodide), and lastly blue fluorescence (Hoëchst 33258).

2.5. Image processing and analysis

Quantitative image analysis was carried out using the software modules supplied with the InCell 3000 (GE Biosciences, NJ). Images were analyzed according to the parameters listed in Table 2. Parameters, particularly dilation and threshold, were chosen so that the area measured for the intensity calculations and the granularity calculations were as close as possible. Parameters were also chosen so that the areas measured using the blue marker (Hoechst dye) and the red marker (propidium iodide) were as close as possible in each analysis. From the calculations, the *I*pos value (average intensity per cell over the threshold), the *N*pos value (number of cells above the threshold), the *F*grains value (average percent of fluorescence localized to granules), and the

*N*grains value (average number of granules per cell) were exported. In order to correct intensities (either for the whole cell or nucleus) so as to only account for the intensity in live cells, the following calculation was used:

$$I_{\text{corrected}} = \frac{I\text{pos}^*_{\text{blue}} N\text{pos}_{\text{blue}} - I\text{pos}^*_{\text{red}}\ N\text{pos}_{\text{red}}}{N\text{pos}_{\text{blue}} - N\text{pos}_{\text{red}}} \quad (1)$$

where blue and red indicate which marker was used for the calculation. The *F*grain value reported by the algorithm is the proportion of fluorescence found in granules multiplied by 1000, so a corrected % granularity in live cells is calculated by:

$$\%\text{granularity} = \frac{F\text{grains}^*_{\text{blue}} I\text{pos}^*_{\text{blue}} N\text{pos}_{\text{blue}} - F\text{grains}^*_{\text{red}} I\text{pos}^*_{\text{red}} N\text{pos}_{\text{red}}}{I\text{pos}^*_{\text{blue}} N\text{pos}_{\text{blue}} - I\text{pos}^*_{\text{red}} N\text{pos}_{\text{red}}} * 100 \quad (2)$$

This equation essentially subtracts the intensity in granules in dead cells from the total intensity in granules and divides by the total intensity in live cells to obtain the proportion of intensity in granules in live cells. An average number of granules in live cells ($N_{\text{corrected}}$) was calculated using the formula below:

$$N_{\text{corrected}} = \frac{N\text{grains}^*_{\text{blue}} N\text{pos}_{\text{blue}} - N\text{pos}^*_{\text{red}} N\text{pos}_{\text{red}}}{N\text{pos}_{\text{blue}} - N\text{pos}_{\text{red}}} \quad (3)$$

Finally, the rate of cell death was calculated by dividing $N\text{pos}_{\text{red}}$ by $N\text{pos}_{\text{blue}}$.

2.6. Fluorescence polarization lipid binding experiments

Small unilamellar vesicles (SUV) were prepared as described previously [29]. Lipid mixtures were dissolved in chloroform to a total concentration of 1.0 mM and divided into 1.0 ml aliquots. The chloroform was removed using a Speed Vac system, and the dried lipids were stored at −20 °C. To make SUVs, the dried lipid mixtures were then resuspended in 1.0 ml phosphate buffered saline, pH 7.2 (PBS; 10 mM phosphate, 150 mM NaCl, pH 7.4), vortexed, and sonicated on ice for 40 min until clear. The lipid vesicle solutions were stored at 4 °C until use. For the fluorescence polarization binding experiments, the 1 mM lipid vesicle stock solution was serially diluted with PBS and transferred to a Greiner 384-well medium binding small volume plate (19 μl lipid solution in each well). Fluoresceinated peptides were added (1 μl per well) from a 4 μM stock for a final concentration of 200 nM in the assay. Fluoresceinated peptide diluted into PBS (without lipid vesicles) was used as a low polarization control. Plates were sealed to prevent evaporation, and incubated for 2 h at room temperature in the dark to allow equilibrium to be reached. Fluorescence polarization (FP) was then measured using the LJL Acquest (Molecular Devices, CA) (G=0.8) or the Victor2V (PerkinElmer, MA) (G=1.07) instruments, with an excitation filter at 484 nm and an emission filter at 530 nm, and settings as indicated by the instrument manufacturer. The raw data for binding to mixed composition or negative vesicles were then divided by the average polarization of the peptide in the presence of an equal concentration of neutral lipid to normalize the polarization scale.

3. Results

3.1. Cellular distribution of CPP peptides in live cells using confocal microscopy

Recently, it has been reported that fixation of cells for confocal microscopy studies causes artificial redistribution of cell-penetrating peptides (CPPs), and therefore, may not accurately depict their cellular uptake and distribution [21–25]. We monitored the uptake of both CPPs and these CPPs conjugated to peptides using an InCell 3000 automated confocal microscope to capture images of their distribution in live cells. For this study, two cell lines were used, U2OS (osteosarcoma) and A431 (epidermoid carcinoma). U2OS cells are commonly used for cellular imaging assays because of their flatness; A431 cells were chosen because they are often used to study epithelial growth factor (EGF) cell signal transduction pathways. Confocal imaging of live cells following incubation with the CPPs revealed significant differences in the uptake characteristics between U2OS and A431 cells, depending on the CPP sequence. In U2OS cells (Fig. 1), the uptake characteristics of the CPPs R_7, R_7W, and pAntp at 37 °C are a mixture of diffuse and punctated distribution. The nuclei were visualized with Hoechst 33258 which appears blue and freely permeates the membranes of live cells. The cells were also incubated with propidium iodide to ensure that the distribution patterns observed were only in live cells. R_7 and R_7W show a mostly diffuse pattern with a small amount of vesicle staining, whereas the pAntp is mostly distributed in vesicles which were found to be mostly perinuclear. A striking difference is observed for the cargo-fused peptides, R_7-DTRL and R_7W-VQD, as compared to the nonconjugated CPP. The uptake of these conjugated CPPs is very low and the peptide is found intracellularly almost exclusively in vesicles. This change in the distribution pattern observed for the fused peptides is particularly remarkable for R_7W-VQD because the CPP R_7W is taken up in a highly diffuse manner, but when it is conjugated to peptide, it is taken up very weakly and in a punctate manner. At 4 °C, there is almost no visible amount of punctate staining observed for all three CPPs, as well as for both R_7-DTRL and R_7W-VQD.

In live A431 cells (Fig. 2) at 37 °C, both punctate and diffuse staining, including nuclear staining, continues to be evident for R_7, but for pAntp and R_7W, there is significant punctate distribution with little or no diffuse staining of the cytoplasm or nucleus. At 4 °C, R_7 shows little diffuse uptake, R_7W shows almost completely diffuse staining of

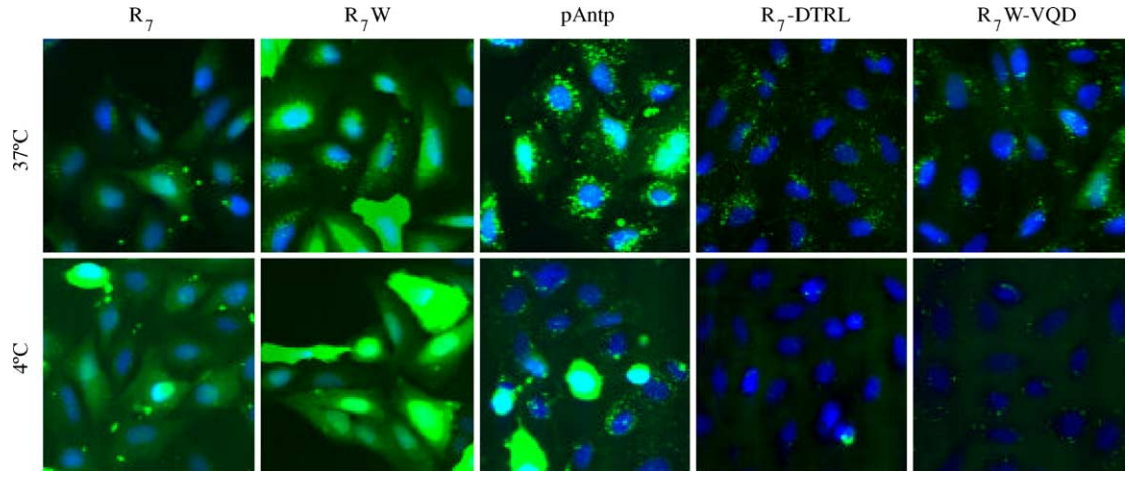

Fig. 1. Cellular uptake of CPP peptides in live U2OS cells. Cells were pre-incubated for 30 min at 37 °C with media containing 5 μM Hoëchst 33258 and 0.12 mg/ml propidium iodide. Peptides were added (10 μM) and cells were incubated for 2 h at either 37 °C or 4 °C, washed twice with PBS, and placed in growth media. Cells were then imaged live on the InCell 3000 confocal microscope. Gains were adjusted for each image to reduce background fluorescence (from no cell area). Fluorescein-labeled peptides are shown in green, and Hoëchst 33258 nuclear stain in blue.

the cytoplasm and nucleus, and pAntp, at this temperature, has much less intense staining that is generally punctate in nature. Similar to the results in U2OS cells, at 37 °C, CPPs conjugated to peptides, R_7-DTRL and R_7W-VQD, show low overall uptake in A431 that is punctate in nature, and at 4 °C, the uptake is barely visible above background. In contrast to the images of fixed cells (data not shown), diffuse uptake of these peptides is not observed in live A431 cells.

3.2. Quantitative analysis of confocal images of live cells

Images obtained from the uptake experiments in live cells were processed using the object intensity and granularity analysis algorithms provided with the InCell 3000 Automated Confocal Microscope. The object intensity algorithm outputs the average fluorescence intensity per cell, while the granularity algorithm calculates the average fluorescence per granule and number of fluorescent granules per cell. In the live cell uptake experiments, both algorithms were used with Hoëchst as the nuclear marker for all cells (because it penetrates both live and dead cells), and with propidium iodide as the nuclear marker for dead cells only (dead cell permeant). By multiplying the cell-average fluorescence by the number of cells detected with each marker, the total green fluorescence intensity of all the live and dead cells in a well (Hoëchst stain) and of all the dead cells in a well (propidium iodide) can be obtained. By subtracting the dead cell fluorescence from the total, and dividing by the number of live cells, it is possible to consider fluorescence only from live cells. In the quantitative analysis, it is preferable to consider only live cells because the dead cells should behave as fixed cells, and as explained previously, the uptake and distribution patterns of CPPs after fixation are different from live cells (data not shown). A similar granularity calculation can be made by considering the total fluorescence from granules using each marker, as well as for the average number of granules per

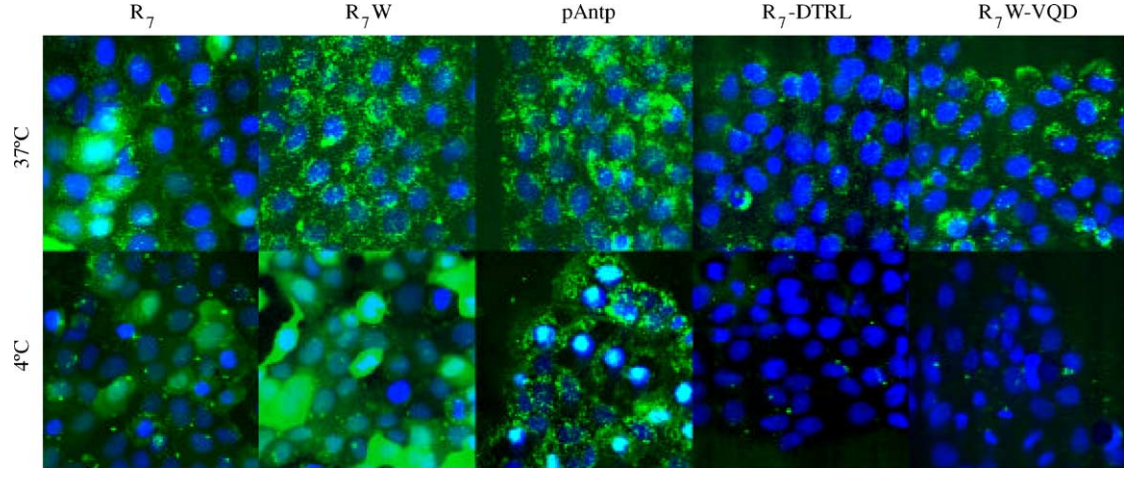

Fig. 2. Cellular uptake of CPP peptides in live A431 cells. Same protocol as described in Fig. 1 was used for A431 cells. Gains were adjusted for each image to reduce background fluorescence (from no cell area). Again, fluorescein-labeled peptides are shown in green, and Hoëchst 33258 nuclear stain in blue.

cell (see Materials and methods). In general, the correction for intensity from dead cells was a small, but under some conditions a large number of cells stained positive with propidium iodide due to toxicity effects of the cell-penetrating peptide.

Quantitative analysis of the confocal images using the InCell 3000 allows for a direct relative comparison of the CPP uptake under different conditions. We first determined that the location of the peptides was indeed intracellular by performing confocal z-scans, which confirmed that the labeled peptides, both when they display diffuse and granular distribution, were located inside the cell and not bound to the extracellular membrane (data not shown). Further confirmation of the intracellular location of the labeled peptides was provided by the demonstration that laser illumination can induce cytoplasmatic redistribution of conjugated CPPs from vesicular compartments [30].

Quantitative analysis of fluorescence from cells and its correlation to cellular distribution after uptake must be used with precaution because of the limitations associated with the algorithm used for the analysis. The first caveat in this analysis is the parameters chosen as input into the algorithms used to calculate the fluorescence values (see Table 2). The final values were chosen for each cell line through an iterative process, optimizing the boundary boxes size to maximize the cell area while minimizing the amount of no cellular background, and also taking into account that most granules were observed to be perinuclear. The parameters used in the algorithm finally depend on cell shape and size, relative size of the nucleus and cytoplasm (A431 cells have a relatively large nucleus), and size of the granules (granules in A431 are much smaller than for U2OS). Once the parameters for the algorithms were established for each cell line, they were kept consistent for the analysis of the uptake of the different peptides in that cell line. Another caveat of the cellular fluorescence analysis is that direct comparison of total cellular peptide uptake by measuring fluorescence intensity is only possible when the cellular distribution of the peptides is similar. This is because fluorescein intensity can decrease in vesicular compartments due to both the acidic pH and self-quenching of the fluorophore. However, by comparing the distribution patterns observed by confocal microscopy and the average fluorescence intensity measured by the InCell 3000, it was observed that the measured average fluorescence intensity of the cells correlates well with the amount of "diffused" peptide distribution. This is illustrated best for R_7W, and pAntp in U2OS cells. By confocal microscopy, R_7W is taken up in a mostly diffuse manner both at 37 °C and 4 °C (Fig. 1), and for this peptide a high fluorescence intensity is measured at both temperatures, >2000 fluorescence units (Fig. 3A). By confocal microscopy, pAntp is taken up mostly in a punctated form (Fig. 1), and low fluorescence intensity is measured, <1000 fluorescence units (Fig. 3A). Therefore, by combining the images and the analysis, it is possible to correlate total measured cellular fluorescence intensity with the degree of diffuse distribution after uptake for each peptide in a cell line.

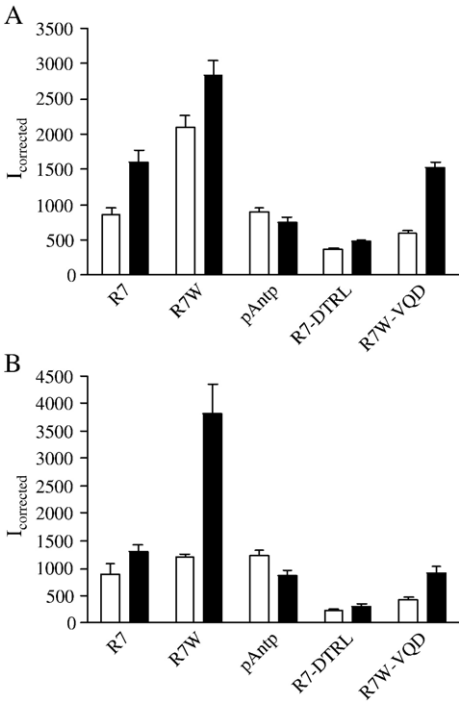

Fig. 3. Quantization of peptide uptake using the object intensity algorithm. Cellular fluorescence intensity was measured as *I*pos, and data are plotted as $I_{corrected}$, calculated as described in Materials and methods. (A) U2OS and (B) A431 cells. Open bar is 37 °C and filled bar is 4 °C.

The average total cellular fluorescence from live cells was calculated as $I_{corrected}$ (Figs. 3A and B). R_7W is the only peptide sequence that shows significant uptake as measured by cellular fluorescence intensity, in both U2OS and A431, and especially at 4 °C. The only other peptide sequence that shows increased fluorescence intensity above 1000 units is R_7 (~1500 units), in both U2OS and A431 cells, but only at 4 °C. The total cellular intensity is also low for pAntp and for R_7 and R_7W conjugated to cargo peptides, R_7-DTRL and R_7W-VQD, for both cell lines and at both temperatures. R_7W-VQD does show higher fluorescence intensity at 4 °C in both cell lines, but this appears to be an artifact of high background staining. There is a good correlation between the fluorescence intensity measurement and the distribution patterns observed (Figs. 1 and 2). For R_7W, there is a clear diffuse pattern after uptake in both cell lines, that is more intense at 4 °C. The rest of the peptides are found mostly in vesicular structures after uptake and that correlates with the very low fluorescence intensity measured, for both cells lines and at both temperatures.

In order to have a direct comparison of the amount of peptide uptake in vesicles, two parameters were calculated, the % granularity (as average percentage of cellular fluorescence from grains, in live cells), and $N_{corrected}$, the average number of fluorescent granules in live cells (Fig. 4). The trends observed using % granularity (average fluorescence from granules per cell) or $N_{corrected}$ (average

number of granules per cell) are essentially the same. In general, it is observed that reducing the temperature generally eliminates or significantly reduces punctate staining of both A431 and U2OS cells. This is also observed in Figs. 1 and 2 and supports the idea that granularity measurements can be used as a quantitative indication of endocytotic peptide uptake, which should be inhibited at low temperatures. The pAntp shows a high degree of granular uptake in both cell lines, compared to the other peptides. R_7W shows high granular uptake in A431 at 37 °C, which confirms the observation in Fig. 2. For U2OS cells at 37 °C, the granularity of uptake of the CPPs conjugated to peptides, R_7-DTRL and R_7W-VQD is comparable to the granularity of uptake of the CPPs alone, whereas in A431 cells the granularity of uptake of R_7-DTRL and R_7 W-VQD is significantly lower than the granularity of uptake of the corresponding CPPs alone. The pAntp peptide exhibits high granularity in both cell lines, and the drop in granularity at 4 °C is very significant.

3.3. Time course of R_7W and pAntp uptake in U2OS cells

R_7W shows high levels of diffuse distribution after uptake in U2OS cells at 37 °C, with some punctate distribution (Figs. 1, 3 and 4). In order to further explore whether these are independent or sequential processes, a time course was carried out to determine their kinetics. Fig. 5A shows a sequence of images for the uptake of R_7W in U2OS at 37 °C, and Fig. 5B shows a plot of the measured fluorescence intensity and granularity. The results indicate that the diffusion process is much faster than vesicle formation, reaching a maximum signal at ~15 min, whereas the maximum granularity is not obtained until 60 min. These data suggest that diffusion and endocytosis occur by either independent mechanisms (diffusion being faster than endocytosis), or sequential processes, by which the peptides are taken up by diffusion first, and then trapped in vesicles. However, since diffusion appears to be observable for at least 2 h and remains fairly constant, independent mechanisms are more favored. In addition, if a similar time course is carried out for the pAntp peptide (Figs. 5A and C), both granularity and diffuse staining appear at a similar rate, further indicating that it is more likely the two distribution modes reflect two mechanistic processes.

3.4. Toxicity of cell-penetrating peptides to live cells

There have not been many studies that address the toxicity of these CPPs in cells. Some reports have indicated that these peptides are non-toxic, and when cytotoxic effects have been seen, it occurs at higher concentrations such as 50 μM [6,22,31]. However, by monitoring the uptake of CPPs in live cell experiments, we found that, at the concentration used in this study, 10 μM, these CPPs are to some extent toxic to cells. Quantitative analysis of the toxicity of the various CPPs under the conditions studied could be obtained using the intensity measurements made

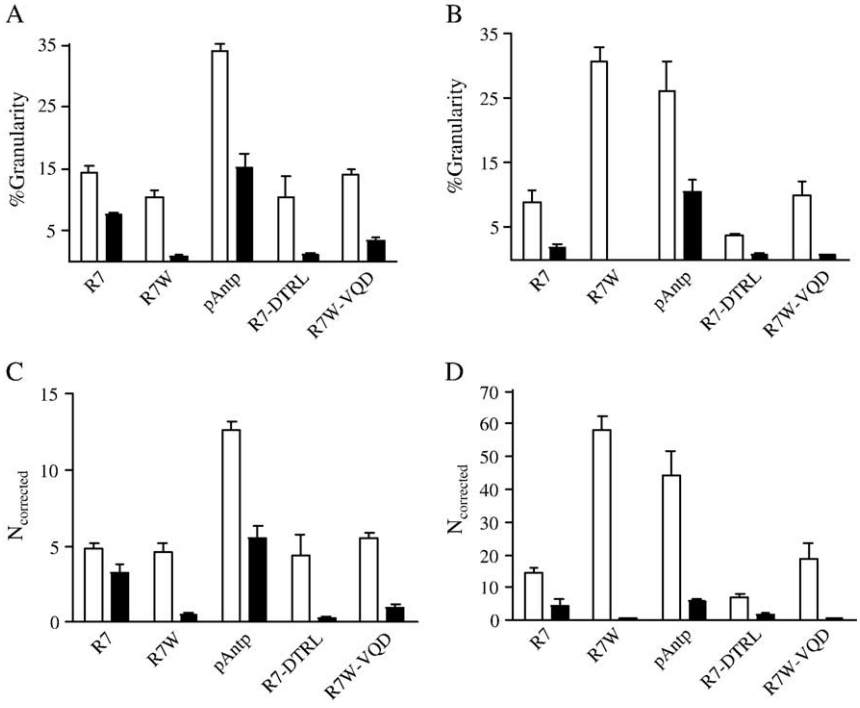

Fig. 4. Quantization of peptide uptake using the granularity algorithm. Granularity was measured from *F*grains and *N*grains, and from these, % granularity and $N_{corrected}$ were obtained as described in Materials and methods, and plotted. % granularity for (A) U2OS and (B) A431 cells. $N_{corrected}$ for (C) U2OS and (D) A431 cells. Open bar is 37 °C and filled bar is 4 °C.

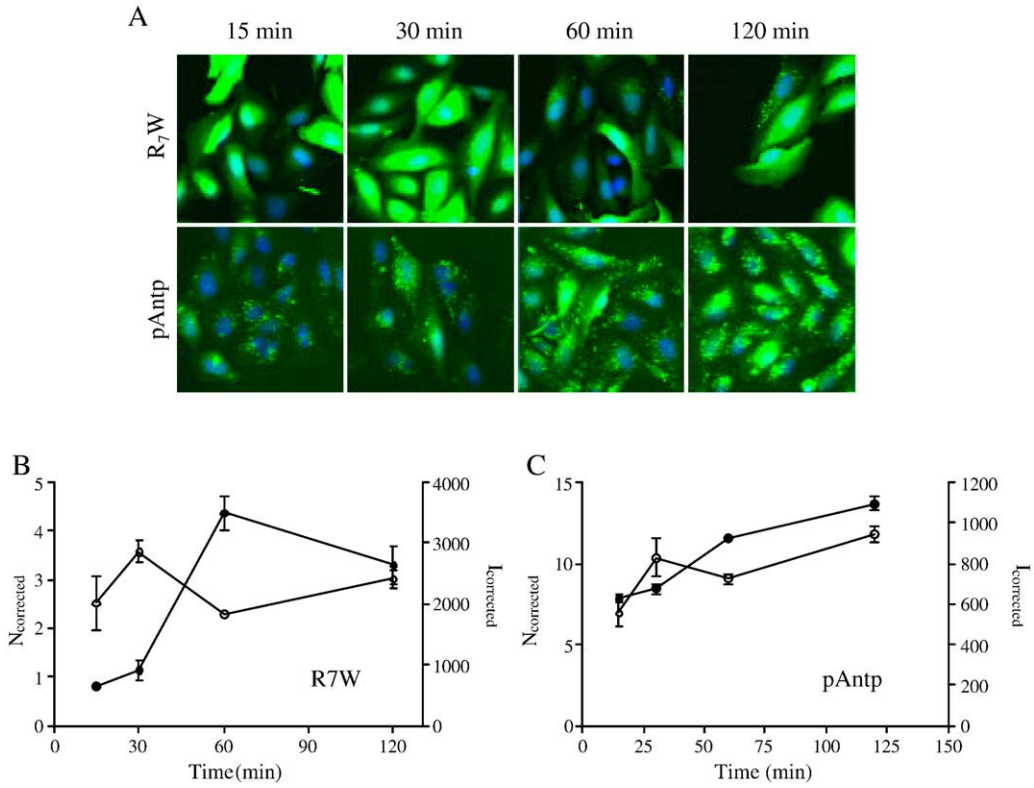

Fig. 5. Time course of R_7W and pAntp uptake in U2OS cells. (A) Confocal images for the cellular uptake of R_7W and pAntp peptides in live U2OS cells. Images were analyzed as described above and uptake quantitated using $I_{corrected}$ (open circles, right y axis) and $N_{corrected}$ (filled circles, left y axis) (B) R_7W uptake (C) pAntp uptake.

with the InCell 3000 confocal microscope. By dividing the number of cells stained with propidium iodide by the number of cells stained with Hoëchst, it is possible to determine the % cell death (Fig. 6). From these data, it was found that R_7 peptide produces the greatest cytotoxicity in both cell types, and that pAntp is also somewhat toxic for U2OS and R_7W for A431, at 4 °C only. The toxicity of the polyarginine peptides, R_7 and R_7W, is enhanced in both cell lines by incubation at 4 °C. This is specially striking for R_7W in A431 cells. In general, the CPPs conjugated to peptides, R_7-DTRL and R_7W-VQD, show very low cytotoxicity. These results suggest a correlation between diffused cellular uptake in the cytoplasm and toxicity because both parameters increase as the temperature is decreased. However, different peptides might have different intrinsic toxicity since the relative amount of diffuse uptake does not correlate with the level of toxicity produced. It is unlikely that lowering the temperature induces cytotoxicity because the control peptide DTRL, which is not fused to a CPP, does not induce cell death at either temperature.

3.5. Binding of CPP peptides to lipid vesicles

In order to ascertain whether the conjugation of peptides to arginine-rich CPPs changes their charge properties in a manner that would effect their uptake by potentially decreasing binding to the cellular membrane, the interaction of fluorescein-tagged CPPs, free and conjugated, with small-unilamellar vesicles (SUVs) was studied by fluorescence polarization (FP). The FP studies were conducted by titrating neutral or negatively charged lipid SUVs against a constant concentration of fluorescein-labeled CPP. In order to compare the binding properties of the different peptides, the fluorescence polarization values measured for the binding of CPPs with negatively charged vesicles or mixed vesicles (30:70 anionic/neutral) were normalized by dividing the average fluorescence polarization of the same peptide in the presence of the same concentration of neutral vesicles to which the peptides do not bind (data not shown). By doing this transformation, the differences in FP signal for each peptide are compensated. The lipid binding characteristics of the peptides varied strongly according to both peptide and lipid vesicle composition. An increase in fluorescence polarization at high concentrations of negative lipid (DMPG or POPG) was observed for all five peptides studied (Figs. 7A and C). All of the peptides bound with lower affinity to the mixed vesicles (Figs. 7B and D) than to the completely negative vesicles (Figs. 7A and C), but the reduction in binding was much smaller for pAntp (on the order of 2-fold) than for the polyarginine peptides. The R_7W peptide displayed the strongest binding to negative lipid vesicles, while the pAntp peptide bound with the greatest affinity to the mixed lipid vesicles. The dramatic change in binding for the

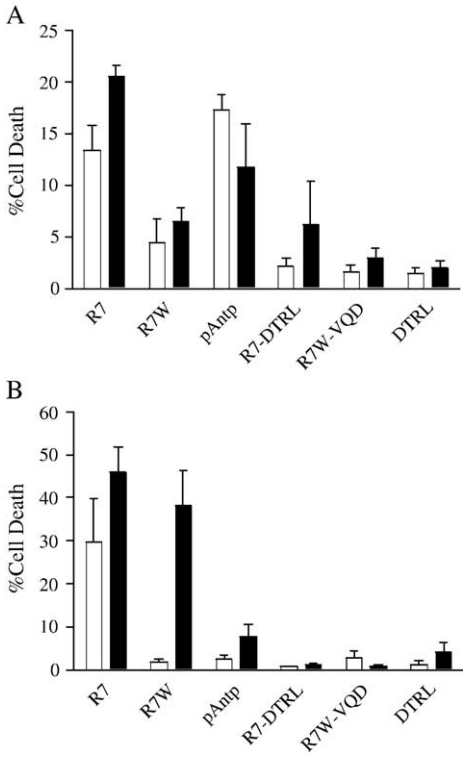

Fig. 6. Toxicity of CPPs to live cells. Percent cell death was calculated by dividing the number of cells staining for propidium iodide by the number of cells staining for Hoëchst 33258. (A) U2OS and (B) A431 cells. Open bar is 37 °C and filled bar is 4 °C.

polyarginine peptides from anionic phospholipids to mixtures of anionic and zwitterionic phospholipids indicates that their interaction with the lipid vesicles is highly charge dependent, whereas the interaction of pAntp appears to be less so. Both arginine-rich CPPs conjugated to peptides, R_7-DTRL and R_7W-VQD, bound to the negatively charged vesicles (Figs. 7A and C). The R_7 and R_7-DTRL peptides appear to bind with similar affinity to the fully negative vesicles, indicating that the addition of a peptide cargo has little effect on the interaction. For the R_7W peptide, however, the binding affinity to anionic vesicles is dramatically reduced by the conjugation of the VQD cargo. The effects of peptide cargo addition to CPPs on lipid binding do not therefore appear to be generally predictable. Since biological membranes are not composed solely of negatively charged lipids, mixed vesicles were used as a more accurate model of membrane composition. Of the peptides studied, pAntp shows significant binding to the mixed vesicles, R_7W appears to have small but detectable binding, and the rest of the peptide sequences do not appear to bind to mixed vesicles (Figs. 7B and D). As a negative control in all lipid binding experiments, the DTRL peptide, which is not fused to a CPP sequence, showed no binding to both anionic and mixed vesicles, indicating the changes in mP measured were indeed due to the restriction in the fluorescein motion upon binding of the CPP sequence to the lipid vesicles.

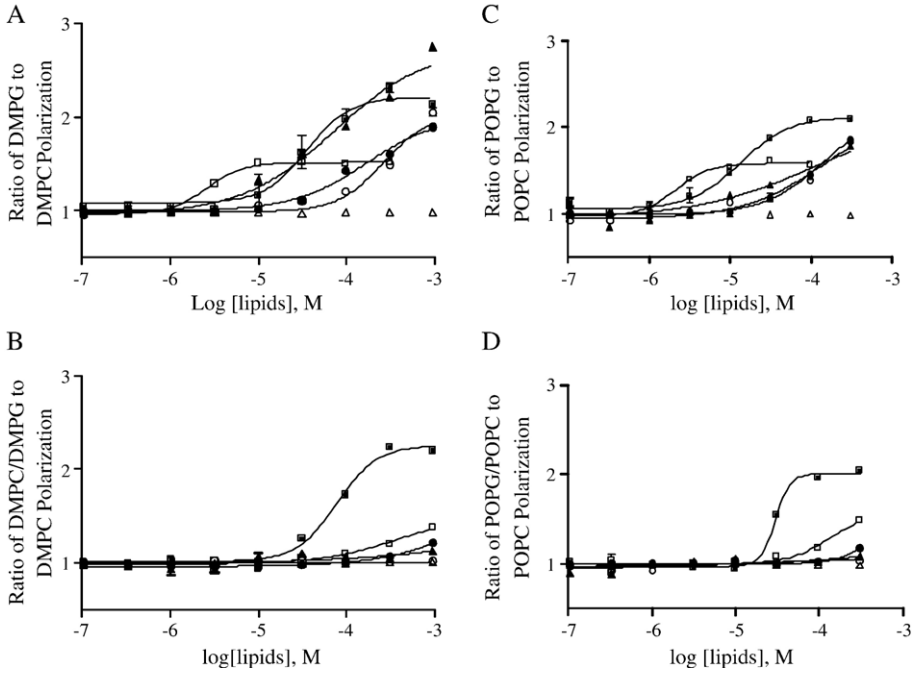

Fig. 7. Binding of cell-penetrating peptides to small unilamellar vesicles (SUVs). Fluorescein-labeled peptides were incubated for 2 h at room temperature in the dark with varying concentrations of lipid SUVs. Binding was measured by fluorescence polarization and the raw data were divided by the average polarization of peptides in the presence of the same concentration of either DMPC (A and B) or POPC (C and D) vesicles. (A) Binding of peptides to DMPG, (B) binding to DMPG/DMPC (30:70), (C) binding to POPG, (D) binding to POPG/POPC (30:70). Filled square, pAntp; open square, R_7W; filled circle, R_7; open circle, R_7-DTRL; filled triangle, R_7W-VQD; and open triangle, DTRL. Data are the mean of at least two independent experiments conducted in triplicate and error bars represent the standard error of the mean (S.E.M.).

4. Discussion

The uptake mechanism and cellular distribution of cell penetrating peptides (CPPs) is not clearly understood, and therefore, their practical use as vectors to import biomolecules into cells might be hindered by the lack of a predictable amount of uptake and cellular distribution. Initial experiments suggested an uptake process leading to a diffused peptide distribution in the cytoplasm which was later found to be an artifact of cell fixation before imaging [21–25]. Recent results in live cells suggest that the uptake mechanism of CPPs is cell and peptide sequence dependent, and it is a combination of direct membrane transport and endocytotic processes [22,25]. In this study, we have combined cellular imaging and quantitative analysis of cellular fluorescence and granular uptake to further investigate the mode of uptake of CPPs and arginine-rich CPPs fused to cargo peptides. Our results suggest that high total average fluorescence intensity correlates with an uptake process leading to diffuse distribution in the cytoplasm, and that granularity measurements are indicative of endocytotic uptake because the extent of granular distribution is mostly eliminated at 4 °C. Here, we have confirmed that in live A431 and U2OS cells, CPPs are taken up in a cell- and sequence-dependent manner. From the imaging results, all of the individual CPPs tested, R_7, R_7W, and pAntp, are taken up in a mixture of diffuse and vesicular distribution in both A431 and U2OS cells. In general, endocytotic uptake is much more prevalent in A431 than in U2OS cells, as measured by the %granularity and the average number of granules per cell. The pAntp peptide is taken up predominately in vesicles by both cell lines, suggesting a mostly endocytotic uptake mechanism, in agreement with results obtained by Thoren et al. [25]. This uptake pattern was found to be in contrast to R_7W which appears to be taken up more efficiently in both cell lines, and in both modes, diffuse and vesicular, for the A431 cells, but significantly more diffuse in U2OS cells, again in agreement with data published previously [25]. R_7 is not taken up very efficiently in either cell line or mode, compared to R_7W, which suggests that the tryptophan residue has an important role in the uptake mechanism. The general loss in granular uptake at 4 °C compared to 37 °C, which is very pronounced for both R_7W and pAntp in A431 cells, supports the hypothesis that the granular uptake is a good measurement of internalization by an endocytotic mechanism.

Most of the mechanistic studies of CPP uptake and distribution in live cells have been carried out using CPPs alone, and not many have looked at the distribution after uptake of CPPs conjugated to biomolecules. A recent study by Console et al. [32] studied the uptake of pAntp and TAT CPPs in complex with avidin or derivatized with phosphatidylcholine liposomes. It was found that these large complexes were internalized into cells and accumulated into vesicular structures, and was reported to be only taken up at 37 °C, supporting an endocytotic uptake mechanism. Another study using TAT–CRE fusion protein [26] has shown rapid internalization by lipid raft-dependent macropinocytosis. Nakase et al. [28] used confocal microscopy and endocytosis inhibitors to study the uptake of arginine-rich peptides fused to an apoptosis-inducing peptide, showing that both the free and conjugated CPP were internalized through an endocytotic route dominated by macropinocytosis. In their studies, Nakase et al. used arginine-rich CPPs fused to a proapoptotic domain peptide, which is an amphiphilic basic peptide, D-$(KLAKLAK)_2$, thus maintaining the highly positive nature of the peptides. In the present study, we fused peptide sequences with negatively charged amino acids to the CPPs to better understand how the ionic nature of the cargo affects the cellular uptake of conjugated CPPs. In our study of live cells, the CPP R_7W showed the most diffuse distribution pattern in the cytoplasm. We were interested to determine if this diffuse pattern would persist with cargo peptides attached since this would be very favorable for studies directed at using peptides to study intracellular signaling pathways in the cytoplasm. Our results show that conjugation of a peptide sequence to the R_7 and R_7W dramatically changes the cellular uptake and distribution of the CPP. When a peptide is fused to R_7W, the total amount of diffused uptake is significantly reduced, and that the small amount of peptide that is taken up is in vesicles. Likewise, when a peptide is fused to R_7, the diffused uptake is greatly reduced, and only a small amount of peptide is taken up, mostly in vesicles. Again, there is a significant decrease in the granular uptake from 37 °C to 4 °C, suggesting an endocytotic uptake.

The process that yields diffuse staining for R_7W in live cells appears to be fast (diffuse staining is evident within 15 min) and appears to occur as well at 4 °C as it does at 37 °C. These results are in agreement with those published by Thorén et al. [25]. Studies have shown that CPP uptake does not permeabilize a lipid bilayer by making holes in it [33,34], and data presented here support this idea because uptake of propidium iodide at 37 °C is not generally observed. Our results from monitoring uptake over time, supports that diffusion and endocytosis occurs by independent mechanisms. For R_7W the total fluorescence intensity of the cell does not significantly decrease as granularity increases. The possibility that peptide is initially internalized by endocytosis and then released into the cytoplasm to cause diffuse staining does not seem be a major pathway in these cell lines because the diffuse staining appears first and the punctate staining later, and it continues to occur at 4 °C when endocytosis is inhibited. Also, for pAntp, which has mainly punctated staining initially, it persists throughout a 2-h time course and does not show the appearance of more diffusion.

In an attempt to explain the different distribution pattern observed after uptake for the arginine-rich CPPs, R_7 and R_7W, compared to their cargo-fused forms, we measured their binding to model membrane systems [29,33,35–37]. All of the peptides bound to the purely negatives vesicles with

relatively similar affinity, and therefore, no correlation between uptake and binding could be obtained. Binding of peptides to mixed vesicles, which might represent a better model of the cell membrane, did not correlate well with uptake either. The pAntp peptide shows the strongest binding to the mixed vesicles but not a strong intensity of uptake in live cells. R_7W, R_7, R_7-DTRL, and R_7W-DTRL are all similar in their binding abilities (detectable for R_7W but not detectable for R_7, R_7-DTRL, and R_7W-DTRL) to the mixed vesicles, but R_7W and R_7 show stronger uptake in live cells. These results suggest that even though additional negative charges on the cargo molecule do not alter binding of the polyarginine peptides to the lipid vesicles significantly, it changes their cellular uptake properties. The results from our study suggest that lipid binding alone cannot explain the uptake characteristics of the peptides. This is in agreement with recent thermodynamic studies that found there is no direct correlation between the lipid-binding characteristics of several CPPs, including pAntp and R_9, and their uptake characteristics [35]. In agreement with the measurements presented here, Thoren at al. showed that the pAntp peptide is a stronger binder to DOPC/DOPG/DSPE-PEG vesicles than R_9. These results also support the idea that heparan sulfate proteoglycans on the surface of cell membrane might play a key role on the uptake of CPPs, and that lipid vesicles might be too simple a cell membrane model to correlate uptake with cell surface binding. The role of heparin sulfate (HS) on the uptake of HIV Tat peptides has been studied for almost a decade [38,39]. Recently, the role of HS on the uptake of polyarginine peptides has been reported, as well [40,41].

In conclusion, the data presented here support the idea that CPPs might be internalized by a combination of mechanisms, one producing a diffuse uptake and another via endocytosis. Whether one or the other mechanism is predominant depends on the CPP sequence, the cargo molecule, and cell type, among other factors. In the two cargo-conjugated arginine-rich CPPs that were studied in this report, endocytosis dominated, and it is conceivable that the effect of different cargo molecules on uptake might vary. Therefore, more work must be conducted in live cells to determine the precise impact of the size and composition of both the CPP and cargo on the cellular uptake and distribution.

Acknowledgements

We thank Mr. Seungtaek Lee (Merck Research Laboratories) for technical help with image acquisition and analysis, and Dr. Berta Strulovici (Merck Research Laboratories) for constant financial support and encouragement.

References

[1] M. Lindgren, M. Hallbrink, A. Prochiantz, Ü. Langel, Cell-penetrating peptides, Trends Pharmacol. Sci. 21 (2000) 99–103.
[2] P. Lundberg, Ü. Langel, A brief introduction to cell-penetrating peptides, J. Mol. Recognit. 16 (2003) 227–233.
[3] E.L. Snyder, S.F. Dowdy, Cell penetrating peptides in drug delivery, Pharmacol. Res. 21 (2004) 389–393.
[4] R. Trehin, H.P. Merkle, Chances and pitfalls of cell penetrating peptides for cellular drug delivery, Eur. J. Pharm. Biopharm. 58 (2004) 209–223.
[5] D. Derossi, A.H. Joliot, G. Chassaing, A. Prochiantz, The third helix of the Antennapedia homeodomain translocates through biological membranes, J. Biol. Chem. 269 (1994) 10444–10450.
[6] E. Vives, P. Brodin, B. Lebleu, A truncated HIV-1 Tat protein basic domain rapidly translocates through the plasma membrane and accumulates in the cell nucleus, J. Biol. Chem. 272 (1997) 16010–16017.
[7] D.J. Mitchell, D.T. Kim, L. Steinman, C.G. Fathman, J.B. Rothbard, Polyarginine enters cells more efficiently than other polycationic homopolymers, J. Pept. Res. 56 (2000) 318–325.
[8] S. Futaki, T. Suzuki, W. Ohashi, T. Yagami, S. Tanaka, K. Ueda, Y. Sugiura, Arginine-rich peptides. An abundant source of membrane-permeable peptides having potential as carriers for intracellular protein delivery, J. Biol. Chem. 276 (2001) 5836–5840.
[9] M. Hällbrink, A. Florén, A. Elmquist, M. Pooga, T. Bartfai, Ü. Langel, Cargo delivery kinetics of cell-penetrating peptides, Biochim. Biophys. Acta 1515 (2001) 101–109.
[10] P.A. Wender, D.J. Mitchell, K. Pattabiraman, E.T. Pelkey, L. Steinman, J.B. Rothbard, The design, synthesis, and evaluation of molecules that enable or enhance cellular uptake: peptoid molecular transporters, Pro. Natl. Acad. Sci. U. S. A. 97 (2000) 13003–13008.
[11] P.A. Wender, J.B. Rothbard, T.C. Jessop, E.L. Kreider, B.L. Wylie, Oligocarbamate molecular transporters: design, synthesis, and biological evaluation of a new class of transporters for drug delivery, J. Am. Chem. Soc. 124 (2002) 13382–13383.
[12] J. Oehlke, A. Scheller, B. Wiesner, E. Krause, M. Beyermann, E. Klauschenz, M. Melzig, M. Bienert, Cellular uptake of an α-helical amphipathic model peptide with the potential to deliver polar compounds into the cell interior non-endocytically, Biochim. Biophys. Acta 1414 (1998) 127–139.
[13] D.J. Dunican, P. Doherty, Designing cell-permeant phosphopeptides to modulate intracellular signaling pathways, Biopolymers (Peptide Science) 60 (2001) 45–60.
[14] D. Derossi, S. Calvet, A. Trembleau, G. Brunissen, G. Chassaing, A. Prochiantz, Cell internalization of the third helix of the Antennapedia homeodomain is receptor independent, J. Biol. Chem. 271 (1996) 18188–18193.
[15] T. Suzuki, S. Futaki, S. Niwa, S. Tanaka, K. Ueda, Y. Sugiura, Possible existence of common internalization mechanisms among arginine-rich peptides, J. Biol. Chem. 277 (2002) 2437–2443.
[16] P.B. Robbins, S.F. Oliver, S.M. Sheu, J.B. Goodnough, P. Wender, P.A. Khavari, Peptide delivery to tissues via reversibly linked protein transduction sequences, BioTechniques 33 (2002) 190–194.
[17] J.B. Rothbard, S. Garlington, Q. Lin, T. Kirschberg, E. Kreider, P.L. McGrane, P.A. Wender, P.A. Khavari, Conjugation of arginine oligomers to cyclosporin A facilitates topical delivery and inhibition of inflammation, Nat. Med. 6 (2000) 1253–1257.
[18] S.R. Scharwze, A. Ho, A. Vocero-Akbani, S.F. Dowdy, In vivo protein transduction: delivery of a biologically active protein into mouse, Science 285 (1999) 1569–1572.
[19] S. Falwell, J. Seery, Y. Daikh, C. Moore, L. Chen, B. Pepinsky, J. Barsoum, Tat-mediated delivery of heterologous proteins into cells, Proc. Natl. Acad. Sci. U. S. A. 91 (1994) 664–668.
[20] A. Astrib-Fisher, D.S. Sergueev, M. Fisher, B.R. Shaw, R.L. Juliano, Antisense inhibition of P-glycoprotein expression using peptide-oligonucleotide conjugates, Biochem. Pharmacol. 60 (2000) 83–90.
[21] S.D. Krämer, H. Wunderli-Allenspach, No entry for TAT(44–57) into liposomes and intact MDCK cells: novel approach to study membrane permeation of cell-penetrating peptides, Biochim. Biophys. Acta 1609 (2003) 161–169.

[22] G. Drin, S. Cottin, E. Blanc, A.R. Rees, J. Temsamani, Studies on the internalization mechanism of cationic cell-penetrating peptides, J. Biol. Chem. 278 (2003) 31192–31201.
[23] J.P. Richard, K. Melikov, E. Vives, C. Ramos, B. Verbeure, M.J. Gait, L.V. Chernomordik, B. Lebleu, Cell-penetrating peptides: a reevaluation of the mechanism of cellular uptake, J. Biol. Chem. 278 (2003) 585–590.
[24] R. Fischer, K. Köhler, M. Fotin-Mleczek, R. Brock, A stepwise dissection of the intracellular fate of cationic cell-penetrating peptides, J. Biol. Chem. 279 (2004) 12625–12635.
[25] P.E.G. Thorén, D. Persson, P. Isakson, M. Goksör, A. Önfelt, B. Nordén, Uptake of analogs of penetratin, Tat(48–60) and oligoarginine in live cells, Biochem. Biophys. Res. Commun. 307 (2003) 100–107.
[26] J.S. Wadia, R.V. Stan, S.F. Dowdy, Transducible TAT-HA fusogenic peptide enhances escape of TAT-fusion proteins after lipid raft macropinocytosis, Nat. Med. 10 (2004) 310–315.
[27] C. Foerg, U. Ziegler, J. Fernandez-Carneado, E. Giralt, R. Rennert, A.G. Beck-Sickinger, H.P. Merkle, Decoding the entry of two novel cell-penetrating peptides in HeLa cells: lipid raft-mediated endocytosis and endosomal escape, Biochemistry 44 (2005) 72–81.
[28] I. Nakase, S. Niwa, T. Takeuchi, K. Sonomura, N. Kawabata, Y. Koike, M. Takehashi, S. Tanaka, K. Ueda, J.C. Simpson, A.T. Jones, Y. Sugiura, S. Futaki, Cellular uptake of arginine-rich peptides: roles for macropinocytosis and actin rearrangement, Mol. Ther. 10 (2004) 1011–1022.
[29] M. Magzoub, L.E.G. Eriksson, A. Gräslund, Conformational states of the cell-permeating peptide penetratin when interacting with phospholipid vesicles: effects of surface charge and peptide concentration, Biochim. Biophys. Acta 1563 (2002) 53–63.
[30] J.R. Maiolo III, E.A. Ottinger, M. Ferrer, Specific redistribution of cell-penetrating peptides from endosomes to the cytoplasm and nucleus upon laser illumination, J. Am. Chem. Soc. 126 (2004) 15376–15377.
[31] C. García-Echeverría, L. Jiang, T.M. Ramsey, S.K. Sharma, Y.P. Chen, A new antennapedia-derived vector for intracellular delivery of exogenous compounds, Bioorg. Med. Chem. Lett. 11 (2001) 1363–1366.
[32] S. Console, C. Marty, C. García-Echeverría, R. Schwendener, K. Ballmer-Hofer, Antennapedia and HIV transactivator of transcription (TAT) "protein transduction domains" promote endocytosis of high molecular weight cargo upon binding to cell surface glycosaminoglycans, J. Biol. Chem. 278 (2003) 35109–35114.
[33] D. Persson, P.E.G. Thorén, M. Herner, P. Lincoln, B. Nordén, Application of a novel analysis to measure the binding of the membrane-translocating peptide penetratin to negatively charged liposomes, Biochemistry 42 (2003) 421–429.
[34] P.E.G. Thorén, D. Persson, M. Karlsson, B. Nordén, The Antennapedia peptide penetratin translocates across lipid bilayers—The first direct observation, FEBS Lett. 482 (2000) 265–268.
[35] P.E.G. Thorén, D. Persson, E.K. Esbjörner, M. Goksör, P. Lincoln, B. Nordén, Membrane binding and translocation of cell-penetrating peptides, Biochemistry 43 (2004) 3417–3489.
[36] A. Ziegler, X.L. Blatter, A. Seelig, J. Seelig, Protein transduction domains of HIV-1 and SIV TAT interact with charged lipid vesicles. Binding mechanism and thermodynamic analysis, Biochemistry 42 (2003) 9185–9194.
[37] M. Magzoub, K. Kilk, L.E.G. Eriksson, Ü. Langel, A. Gräslund, Interaction and structure induction of cell-penetrating peptides in the presence of phospholipid vesicles, Biochim. Biophys. Acta 1512 (2001) 77–89.
[38] M. Rusnati, D. Coltrini, P. Oreste, G. Zoppetti, A. Albini, D. Noonan, F. d'Adda di Fagagna, M. Giacca, M. Presta, Interaction of HIV-1 tat protein with heparin, J. Biol. Chem. 272 (1997) 11313–11320.
[39] M. Tyagi, M. Rusnati, M. Presta, M. Giacca, Internalization of HIV-1 tat requires cell surface heparan sulfate proteoglycans, J. Biol. Chem. 276 (2001) 3254–3261.
[40] S.M. Fuchs, R.T. Raines, Pathway for polyarginine entry into mammalian cells, Biochemistry 43 (2004) 2438–2444.
[41] E. Goncalves, E. Kitas, J. Seelig, Binding of oligoarginine to membrane lipids and heparan sulfate: structural and thermodynamic characterization of a cell-penetrating peptide, Biochemistry 44 (2005) 2692–2702.